Proceedings of the 28th IEEE
EMBS Annual International Conference
New York City, USA, Aug 30-Sept 3, 2006

Separation of Subcortical Component from Cortical Auditory Evoked Potential by Independent Component Analysis

Hirokazu Takahashi, Masayuki Nakao, and Kimitaka Kaga

***Abstract*—Auditory evoked potentials (AEPs) in the temporal cortex have typical slow positive/negative (P1/N1) biphasic waves, which are occasionally associated with an additional earlier small deflection (P0/N0). In the present paper, we attempted to address the neural origin of P0/N0 deflection by the independent component analysis (ICA) of densely mapped cortical AEPs of rats. The ICA results suggest that the deflection appears when subcortical contribution to AEP is equal to or larger than cortical contribution.**

I. Introduction

External stimuli activate multiple regions in the brain, each of which produces different evoked potentials. Auditory evoked potentials (AEPs) in the temporal cortex and vertex exhibit different waveforms. The temporal AEP of rat, guinea pig, and cats have typical slow positive/negative biphasic waves (P1/N1) within 50-ms post-stimulus latency, which are occasionally associated with an additional earlier small deflection (P0/N0) [1]-[6]. The vertex AEP also has several typical waves, which are different from temporal waves [6]-[8]. Previous extensive studies of cortical mapping and cortical inactivation suggested that P1/N1 waves have neural origins in the auditory cortex and that the vertex AEP has subcortical origins. However, the origin of P0/N0 waves has not been satisfactorily understood to date.

The short latency of P0/N0 can be considered a sign of a subcortical origin. In contrast, cortical inactivation affected the early components [3], and depth recording found a short-latency large deflection in a deep cortical laminate [5], [9], suggesting that P0/N0 has a cortical origin. These contradictions have led to a multiple origin hypothesis [3], [5]-[7]. In these past studies, separate discussions of the temporal and vertex AEPs may have overlooked the P0/N0 origin.

In order to better understand the controversial AEP neural origins, the present study attempts the independent component analysis (ICA) to separate subcortical and cortical contributions from densely mapped temporal AEPs of rats.

II. Material and Method

We anesthetized 10 rats with pentobarbital (50 mg/kg; IP) and another 10 rats with ketamine (60 mg/kg; IM) and xylazine (5 mg/kg; IM), and mapped AEPs epidurally with a surface microelectrode array [10]. We also epipially mapped AEPs for the ketamine-xylazine anesthetized rats. The array had 32 recording points within 2 mm by 2 mm, which covered the primary auditory cortex. Clicks at 80 dB SPL and tone bursts at 70 dB SPL served as test stimuli, which were calibrated with a microphone at the entrance of the ear. Cortical AEPs were simultaneously amplified with a gain of 1000 and filtered with a band pass of 20 – 1500 Hz, -12 dB/octave, and digitized at a sampling rate of 5 kHz. All the data presented were the average after taking 50 trials or more. Detailed procedures for the AEP measurement with a surface microelectrode array are described elsewhere [1], [10].

We ran FastICA of the measured AEP map [11]. Taking n point AEP data $x(t)$ (usually $n = 32$) as a linear combination of m dimensional independent components $s(t)$ and n by m "mixing matrix" $\mathbf{A}$ (*i.e.*, $x(t) = \mathbf{A}s(t)$), ICA optimizes an arbitrary "unmixing matrix" $\mathbf{W}$ so that each signal of $\hat{s} = \mathbf{W}x$

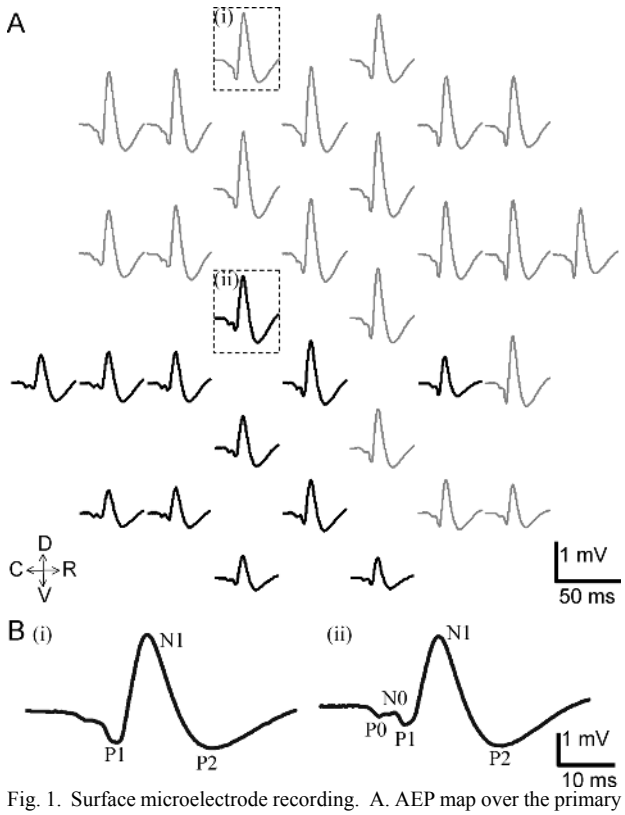

Fig. 1. Surface microelectrode recording. A. AEP map over the primary auditory cortex by ketamine-xylazine-anesthesia epidural recording. Each waveform is approximately aligned in the spatial coordinates of recording sites. Bold waveforms are judged as having a P0/N0 deflection. R, rostral; C, caudal; D, dorsal; V, ventral. B. Definitions of wave.

H. Takahashi is with Graduate School of Information Science and Technology, the University of Tokyo, Tokyo, 153-8904, Japan (corresponding author to provide phone/fax: +81-5452-5196; e-mail: takahashi@i.u-tokyo.ac.jp).

M. Nakao is with Graduate School of Engineering, the University of Tokyo, Tokyo, 113-8656, Japan.

K. Kaga is with Graduate School of Medicine, the University of Tokyo, Tokyo, 113-8655, Japan.

becomes as independent as possible. Practically, ICA used a fixed-point iteration and maximized the following contrast function $\boldsymbol{J}$ under $\| \boldsymbol{w}_i \| = 1$:

$$\boldsymbol{J} = [\boldsymbol{E}\{\boldsymbol{G}(w_i^t)\} - \boldsymbol{E}\{\boldsymbol{G}(\nu)\}],$$

$$\boldsymbol{G}(u) = \log \cosh(u),$$

where $\boldsymbol{E}\{\boldsymbol{X}\}$ is the expectation value of $\boldsymbol{X}$, w is one of the row vectors of **W**, and ν is a standardized Gaussian variable. The mixing matrix **A** can then be obtained as the inverse of the unmixing matrix **W**. In the preprocessing of ICA, we first centered and whitened AEP data, and reduce the data dimension to m by PCA, *i.e.*, determine the number of ICs. Since each of obtained ICs, $\hat{s}$, has also been centered and whitened, each column of the mixing matrix (*i.e.*, n dimensional vector) represents a contribution of each IC to the corresponding AEP.

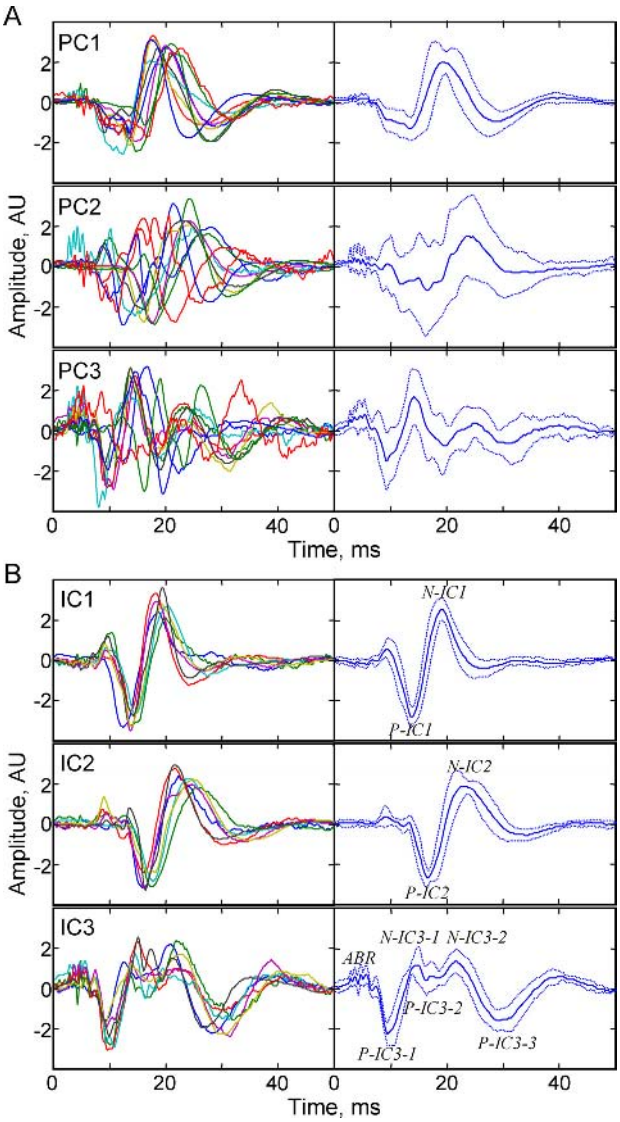

Fig. 2. PCA and ICA of AEPs of pentobarbital-anesthesia epidural recording. A. Principle components. B. Independent components and definition of characteristic wave. Left insets show components obtained form an individual animal, and right insets show the grand-average (solid line) and standard deviation (dotted line).

III. Results

Figure 1A shows click-evoked AEPs mapped over the primary auditory cortex, and Fig. 1B defines the AEP waves. We identified P0/N0 waves when P0-N0 amplitude was larger than 10% of P1 amplitude. Total numbers of measured AEP were 277, 312, and 320 from each of 10 rats for pentobarbital- anesthesia epidural recording, ketamine-xylazine-anesthesia epidural recording, and ketamine-xylazine-anesthesia epipial recording, respectively. P0-N0 was identified in 10, 4, and 0 animals for each recording. Total numbers (and probability of appearacne) of identified P0/N0 were 134 (49.4%), 57 (17.8%), and 0 (0%) for each recording. The amplitudes of P1/N1 waves were 0.20, 1.8, and 3.8 mV on average for each recording. Pentobarbital anesthesia significantly reduced AEP amplitude as compared to ketamine-xylazine anesthesia.

Figure 2A shows 1st to 3rd principle components (PCs) for pentobarbital-anesthesia epidural recording. The contributing rates (and the standard deviations) of 1st to 5th PCs were 92.4 (4.1), 5.99 (4.13), 1.08 (0.66), 0.24 (0.13), and 0.09% (0.04%), respectively. On the basis of this result, IC number n was initially selected between 2 and 4, and trial-and-error ICA application finally determined an optimal number, with which ICA can best separate subcortical responses. In 8 out of 10 rats, the optimal number of IC was 3, with which ICA could separate a putative subcortical component with clear auditory brainstem responses (ABRs) within 10-ms post-stimulus latency and subsequent vertex-AEP-like slow waves [6]-[8]. We labeled this subcortical component as IC3 and 2 other biphasic components as IC1 and IC2 according to the latency (Fig. 2B). Similar ICs were also identified for ketamine-xylazine-anesthesia epidural recording, although ABR was too small to be identified (Fig. 3).

For cortices that exhibit P0/N0 waves, we examined the obtained mixing matrix **A** and plotted contributions of each IC to AEP in order to find significant combinations of the

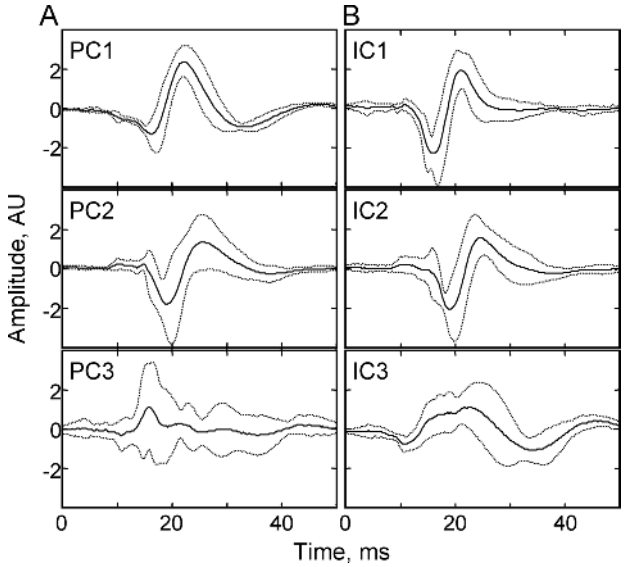

Fig. 3. Grand-averaged PCs and ICs of AEPs of ketamine-xylazine-anesthesia epidural recording. See Fig. 2 for conventions.

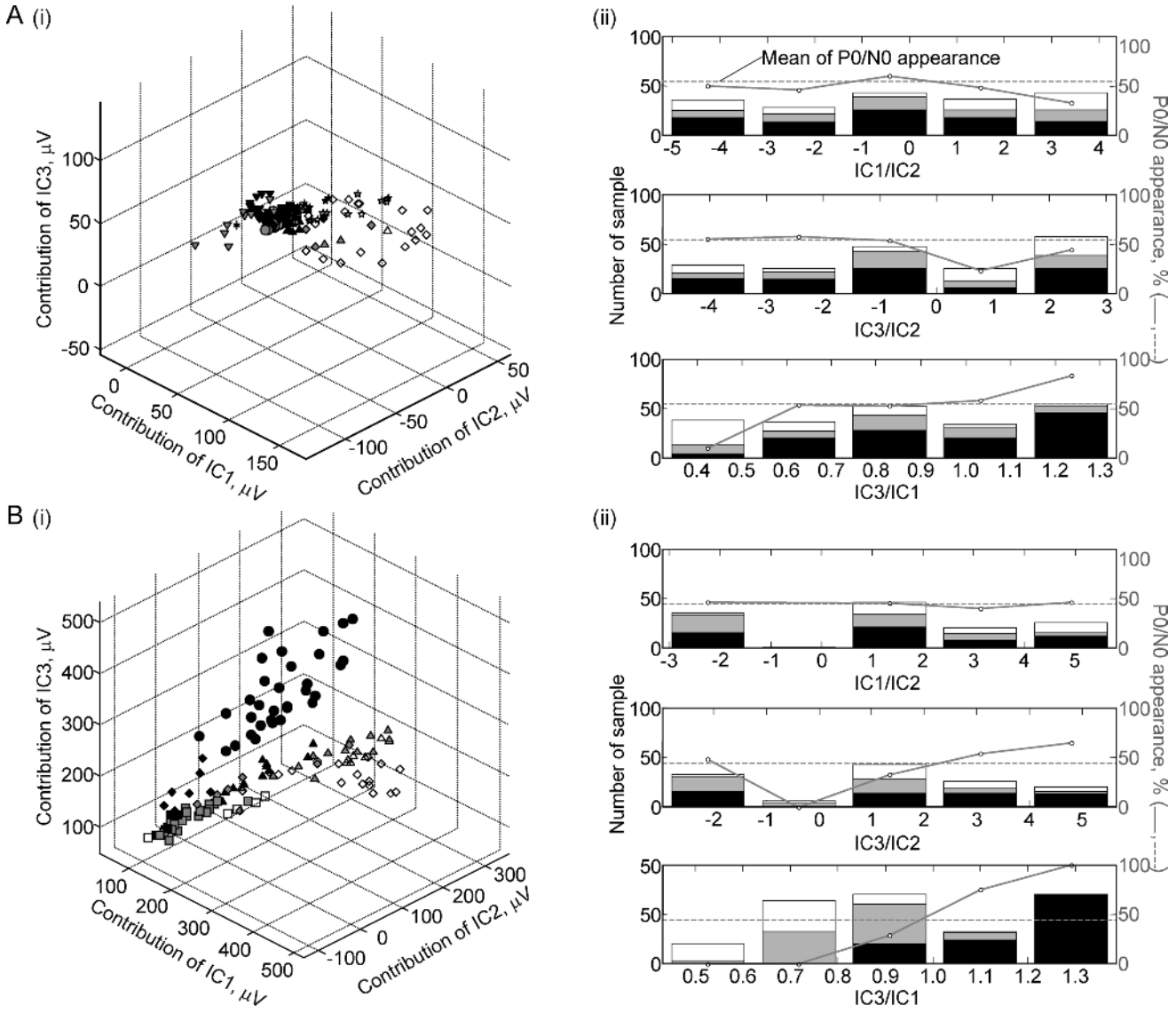

Fig. 4. Condition for P0/N0 appearance. A. Pentobarbital-anesthesia epidural recording. B. Ketamine-xylazine-anesthesia epidural recording. (i), contribution of each IC to AEP. Each marker type indicates AEP from an identical animal. Marker colors indicate P0/N0 amplitude: black, 10% or more of P1 amplitude; grey, 1 – 10% of P1 amplitude; white, 1% or less of P1 amplitude. (ii), P0/N0 appearance as a function of combination of each IC contribution. Histograms show the distributions of the proportions between indicated IC contributions. Each bar is multicolored with colors corresponding to P0/N0 amplitude as defined in (i). Line plots also indicate frequencies of P0/N0 appearance.

contribution that could produce P0/N0 wave (Fig. 4). We could not find any general relationship between each IC contribution and P0/N0 appearance across the recording conditions. We then investigated the proportions of each IC contribution to other IC contribution. For both pentobarbital-anesthesia and ketamine-xylazine-anesthesia epidural recording, P0/N0 appears significantly frequently when IC3/IC1 > 1.

We finally applied ICA to tone-evoked AEPs, and obtained 3 typical ICs (Fig. 5A), which were identical to ICs of click-evoked AEPs. Figure 5B reconstructed the areal distributions of each IC contribution. IC1 typically exhibited a focal distribution, and the location of the focus depended on the test frequency of tones. These foci almost matched a place code of frequency in the auditory cortex, *i.e.*, tonotopic organization [1], suggesting that IC1 reflects a direct thalamo- cortical input. IC2 and IC3, on the other hand, have less focal distribution, and a significant proportion have almost flat distribution.

IV. Discussion

Our results suggest that the temporal AEP consists of at least 3 components with independent origins. The tonotopic representation of IC distribution (Fig. 5) suggests that IC1 possibly reflected mainstream thalamo-cortical inputs (*i.e.*, projection from ventral portion of medial geniculate body (MGB)) [4]-[7]. The characteristics of a waveform suggest that IC3 can be considered subcortical activities. Notably, for pentobarbital- anesthesia epidural recording, ABRs were clearly identified in IC3 (Fig. 2). The latencies of other slow characteristic waves suggest that IC3 reflects the vertex AEP.

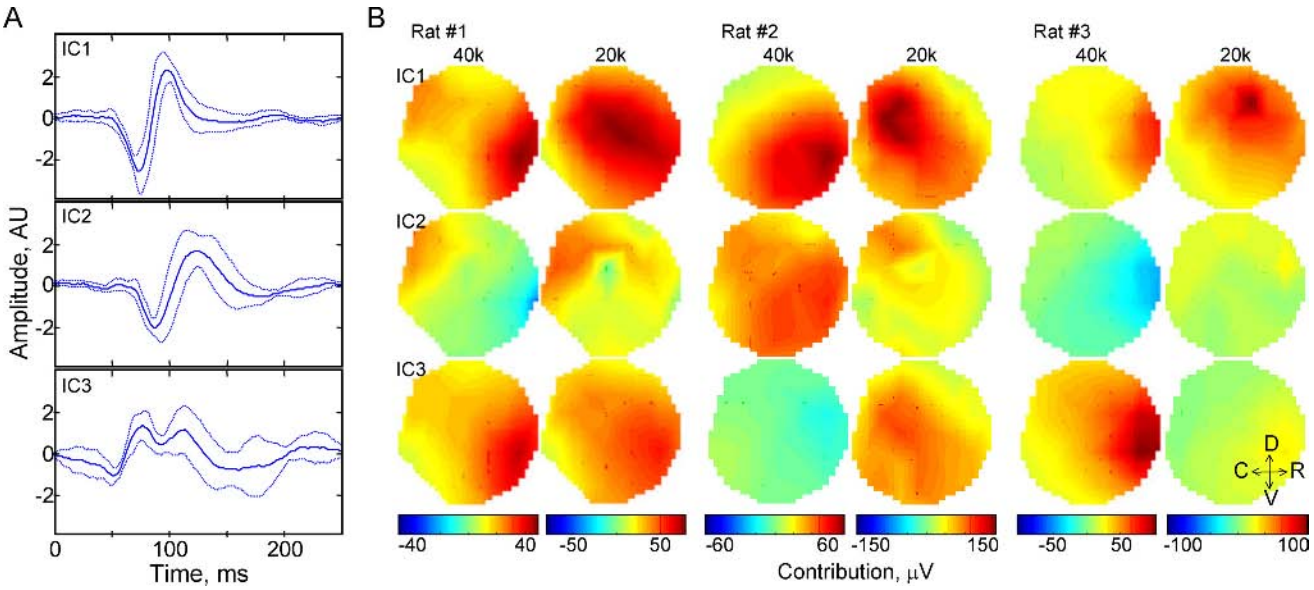

Fig. 5. ICA of tone-evoked AEPs. A. Grand-averaged ICs. See Fig. 2 for conventions. B. Areal distributions of each IC contribution. The recording area covered the primary auditory cortex, where low-frequency (20-kHz) tones activate caudal loci and high-frequency (40-kHz) tones activate rostral loci.

The origin of IC2 remains unknown. The delay of 2.5 – 5 ms from IC1 may imply that IC2 reflects cortico-cortical inputs. Alternatively, IC2 may reflect sidestream thalamo-cortical inputs (*i.e.*, projection from dorsal portion of MGB) [4].

Previous studies often employed PCA for multiple evoked potentials [5], [9]. PCA, however, operates under the strict constraint that components must be orthogonal to one another. This mathematical constraint may not hold in many physiological phenomena, resulting in an obscure interpretation. On the other hand, ICA with the constraint of independence reflects some biological phenomena more realistically. This difference may distinguish the interpretable ICs from the hardly explainable PCs (Fig. 2).

The early deflection P0/N0 generally appeared when subcortical IC3 contribution is equal to or larger than cortical IC1 contribution (Fig. 4). In terms of latencies, an adequate combination of P-IC1 and P-IC3-1 is obviously crucial for the formation of P0/N0. Consistent with our idea, ketamine-xylazine-anesthesia epipial recording could not find P0/N0 waves because the recoding reflected cortical activities predominantly as compared to other recordings. Thus, significant contributions from both cortical and subcortical activities might confound the P0/N0 origins previously.

In clinical screenings, auditory, visual, and somatosensory evoked potentials are routinely obtained with epicranial electrodes [12]. Similar to rat AEP we focused so far, these human evoked potentials also exhibit characteristic waves, some of which have unclear origins and are again discussed within the multiple origin hypothesis. Epicranially measured evoked potentials equally mix subcortical and cortical contributions because distances from electrodes to cortical sources approximate distances to subcortical sources. In such conditions, our idea is specifically worth considering for the identification of these controversial origins.

REFERENCES

[1] H. Takahashi, M. Nakao, and K. Kaga, "Interfield differences in intensity and frequency representation of evoked potentials in rat auditory cortex," *Hear. Res.*, vol. 210, 2005, pp. 9-23.

[2] K. Kaga, R. F. Hink, Y. Shinoda, and J. Suzuki, "Evidence for a primary cortical origin of the middle latency auditory evoked potential in cats," *Electroencephalogr. Clin. Neurophysiol.*, vol. 50, 1980, pp. 254-266.

[3] G. V. Simpson, and R. T. Knight, "Multiple brain system generating the rat auditory evoked potential. I. Characterization of the auditory cortex response," *Brain Res*., vol. 602, 1993, pp. 240-250.

[4] S. Di, and D. S. Barth, "The functional anatomy of middle-latency auditory evoked potentials, Thalamocortical connections," *J. Neurophysiol*, vol. 68, 1992, pp. 425-431.

[5] D. S. Barth, and S. Di, "Three-dimensional analysis of auditory-evoked potentials in rat neocortex," *J. Neurophysiol.*, vol. 64, 1990, pp. 1527-1536.

[6] T. McGee, N. Kraus, C. Comperatore, and T. Nicol, "Subcortical and cortical components of the MLR generating system," *Brain. Res.*, vol. 544, 1991, pp. 211-220.

[7] G. V. Simpson, and R. T. Knight, "Multiple brain system generating the rat auditory evoked potential. II. Dissociation of auditory cortex and non-lemniscal generator system," *Brain Res*., vol. 602, 1993, pp. 251-253.

[8] L. S. Kim, K. Kaga, T. Tsuzuku, and A. Uno, "Effects of primary auditory cortex lesions on middle latency responses in awake cats," *Auris Nasus Larynx*, vol. 20, 1993, pp. 155-165.

[9] M. Steinschneider, C. E. Tenke, C. E. Schroeder, D. C. Javitt, G. V. Simpson, J. C. Arezzo, and H. G. Vaughan Jr, "Cellular generators of the cortical auditory evoked potential initial component," *Electroencephalogr. Clin. Neurophysiol.*, vol. 84, 1992, pp. 196-200.

[10] H. Takahashi, T. Ejiri, M. Nakao, M. Nakamura, K. Kaga, and T. Hervé, "Microelectrode array on folding polyimide ribbon for epidural mapping of functional evoked potentials," *IEEE Trans. Biomed. Eng.*, vol. 50, 2003, pp. 510-516.

[11] A. Hyvärinen, and E. Oja, "Independent component analysis: algorithms and application," *Neural Networks* vol. 12, 1999, pp. 411-430.

[12] T. W. Picton, S. A. Hillyanrd, H. I. Krausz, and R. Galambos, "Human Auditory evoked potentials. I: Evaluation of Components," *Electroencephalogr. Clin. Neurophysiol.*, vol. 36, 1974, pp. 179-190.